

CHROMSYMP 1118

## CHARACTERIZATION OF PEAK ASYMMETRY WITH OVERLOADED CAPILLARY COLUMNS

ALAIN JAULMES\*, IOANNIS IGNATIADIS, PHILIPPE CARDOT and CLAIRE VIDAL-MADJAR\*

*Ecole Polytechnique, Département de Chimie, Laboratoire de Chimie Analytique Physique, Route de Saclay, 91128 Palaiseau Cedex (France)*

---

### SUMMARY

A theoretical model for elution peaks (based on the solution of the mass-balance equations with a parabolic expansion of the isotherm equation) is in good agreement with the experimental peak profiles observed in capillary gas chromatography. It depends on four parameters: the peak area, the limiting retention time at zero concentration, the global apparent diffusion coefficient, and the peak slant coefficient. The sorption effect, which is a flow-rate increase inside the solute band, has a back-leaning, asymmetrical effect. It is a major contribution to the peak distortions observed in capillary gas chromatography. It is shown that one of the parameters of the theoretical model, the proportionality factor  $\mu_0$ , is characteristic of peak asymmetry and is easily measured from the variation of peak maximum with the amount injected. The asymmetry depends greatly on the magnitude of the second derivative of the isotherm at the origin. It is due to column overloading and is independent of column length and flow-rate. It increases with decreasing column diameter and with decreasing film thickness. This proportionality factor is useful for characterizing the degree of asymmetry of capillary columns, especially for comparing the stationary phases and the coating procedures.

---

### INTRODUCTION

The concentration profiles observed in capillary gas-liquid chromatography often differ from the ideal Poisson distribution law on which the plate height model is based. At infinite dilution, the experimental peaks are well described by the exponentially modified Gaussian<sup>1,2</sup>. In this case peak distortions are only due to extra-column effects, such as dead-volume contributions. Other mathematical expressions<sup>3,4</sup> have been introduced to explain strongly tailing peaks in the case of a linear sorption isotherm. However, in capillary gas chromatography, asymmetrical peaks

---

\* Present address: CNRS, Laboratoire de Physico-Chimie des Biopolymères, 2, rue Henri Dunant, 94320 Thiais Cedex, France

with front-leading edges are generally observed, which are due to column overloading. Theoretical models<sup>5-7</sup> that take into account the non-linearity of the equilibrium isotherm are therefore needed to describe the experimental elution profiles observed in gas chromatography for large amounts injected.

## THEORY

When equilibrium is achieved for the distribution of the solute between the carrier gas and the stationary phase, the mass-balance equation of the chromatographic system for the solute is

$$\frac{\partial X}{\partial t} (1 + k') + \frac{\partial(uX)}{\partial z} = D \frac{\partial^2 X}{\partial z^2} \quad (1)$$

and for the carrier gas, it is

$$\frac{\partial X}{\partial t} = \frac{\partial[u(1 - X)]}{\partial z} - \frac{\partial^2 X}{\partial z^2} D \quad (2)$$

where  $X$  is the mole fraction of the solute in the gas phase,  $t$  is the time,  $z$  the abscissa along the column,  $u$  the local velocity of the mobile phase,  $k'$  the solute capacity factor, and  $D$  the apparent diffusion coefficient in the gas phase.

The capacity factor,  $k'$ , is related to the isotherm equation, which describes the equilibrium between the stationary phase and the mobile phase

$$k' = (\partial n_A^S / \partial n_A^G)_p \quad (3)$$

where  $n_A^S$  and  $n_A^G$  are the number of moles of solute A in the stationary phase and in the gaseous phase, respectively.

The system of mass-balance equations which describes the flow-rate perturbation caused by large solute concentrations (eqn. 2) cannot be solved directly without further simplifications. We have shown previously<sup>5</sup> that the set of mass balance equations can be simplified, if we assume (i) the mole fraction of the solute to be negligible compared to that of the carrier gas and (ii) a constant (mean) pressure  $\bar{p}$  throughout the column. In that case we obtain:

$$\frac{\partial C}{\partial t} (1 + k') + u_0(1 - \lambda_s C) \frac{\partial C}{\partial z} = D \frac{\partial^2 C}{\partial z^2} \quad (4)$$

where  $C$  is the concentration of solute in the carrier gas,  $u_0$  the outlet carrier-gas velocity,  $\lambda_s$  a corrective factor which describes the contribution of the sorption effect<sup>8</sup>:

$$\lambda_s = - \frac{2k'_0 RT}{(1 + k'_0)\bar{p}} \quad (5)$$

where  $k'_0$  is the limiting value of the solute capacity factor at zero sample size,  $R$  the gas constant, and  $T$  the column temperature.

Houghton<sup>9</sup> has shown that an analytical expression for the elution profile can

be obtained by solving eqn. 4 for a small non-linearity of the sorption isotherm when  $k'$  is expanded to its second term:

$$n'_\lambda/V_S = \alpha C + \beta C^2/2 \tag{6}$$

where  $V_S$  is the volume of stationary phase. Therefore

$$k' = k'_0 + k''_0 V_0 C \tag{7}$$

where  $V_0$  is the volume of the gaseous phase,  $k'_0 = \alpha V_S/V_0$ , and  $k''_0 = \beta V_S/V_0^2$ .

For a Dirac injection function we have shown<sup>5</sup> that the expression of the elution peak profile is

$$C = \frac{2}{\lambda U} \left( \frac{D'}{\pi t} \right)^{1/2} \frac{\exp\left(-\frac{\xi^2}{4D't}\right)}{\coth\left(\frac{\mu}{2}\right) + \operatorname{erf}\left[\frac{\xi}{2(D't)^{1/2}}\right]} \tag{8}$$

the right-hand side of eqn. (8) is determined by 4 parameters:

(i) the peak size parameter,  $a$ , corresponding to the effective peak area  $A_T$  for small sample sizes,

(ii) the slope of the isotherm at origin  $k'_0$ , which is related to the retention time at infinite dilution,  $t_R$ , and to the retention time of an unretained peak,  $t_0$ :

$$t_R = (1 + k'_0)t_0 \tag{9}$$

(iii) the global apparent diffusion coefficient,  $D' = D/(1 + k'_0)$ , which is related to the standard deviation,  $\sigma_0$ , of a Gaussian peak and to the column length,  $L$

$$\sigma_0 = t_R \sqrt{2D't_R} / L \tag{10}$$

(iv) the curvature of the isotherm at the origin,  $k''_0$ , which is related to the peak slant coefficient,  $\lambda$ :

$$\lambda = \frac{k''_0 V_0}{1 + k'_0} + \lambda_S \tag{11}$$

The other auxiliary variables are:

$$U = L/t_R = u_0/(1 + k'_0) \tag{12}$$

$$\xi = L - Ut \tag{13}$$

$$\mu = a\lambda U^2/2D' = a\lambda t_R/\sigma_0^2 \tag{14}$$

A simple relationship exists between the coordinates  $t_M$  and  $C_M$  of the peak maximum

$$C_M = (t_M - t_R)/\lambda t_M \quad (15)$$

This equation corresponds to a hyperbola, and the values of  $t_R$  and  $\lambda$  may be determined by linear regression from the plot of  $1/t_M$  vs.  $C_M$ :

$$1/t_M = \lambda C_M/t_R + 1/t_R \quad (16)$$

Eqn. 15 reduces to a straight line for small values of  $C_M$ :

$$C_M \approx (t_M - t_R)/\lambda t_R \quad (17)$$

## EXPERIMENTAL

The chromatographic equipment previously described<sup>6</sup> and specially designed for this type of work incorporates a fluid sample switch injector and a flame-ionization detector (Carlo Erba, Milan, Italy). The whole system is placed in an air-stirred oven (Servomex, Crowborough, U.K.), the temperature of which is maintained within 0.1°C with a proportional and integral controller.

The "fluidic logic" injector design of Gaspar *et al.*<sup>10</sup> was used in this study, in order to obtain symmetrical, reproducible injection profiles, the width of which (30 ms) does not change when the amount of sample injected into the column is increased. The general injection system, which includes a bistable fluidic logic gate (Model 191454, Corning Glass, NY, U.S.A.), has been previously described<sup>6</sup>. The fluidic device is enclosed in a pressurized vessel.

The column is connected to this injection system. The command pulse is actuated by a solenoid valve (Clippard EVO-3, Cincinnati, OH, U.S.A.) for a time which can be chosen between 10 and 100 ms. The connections between the command inlets (ports) allow attainment of a rectangular injection profile of constant duration (30 ms throughout this work). The solute (liquid sample) is injected manually and vaporized in a stream of nitrogen and methane, which carries the vapours to the fluidic gate.

In order to measure reliable values of  $k'$ , a mixture of methane and solute vapours was injected into the column. Methane was used to determine the gas hold-up time,  $t_0$ , since it is the least adsorbed gas that gives a signal with the flame ionization detector.

The fused-silica capillary column, 20 m × 0.25 mm I.D. (SGE, Melbourne, Australia), was coated with OV-73 (5.5% phenyl-94.5% methylsilicone from Applied Science Labs., PA, U.S.A.) according to a procedure previously described<sup>7</sup>, and the film thickness was approximately 0.2 μm. Helium was used as the carrier gas. The pressure drop was controlled by a pressure regulator (Texas Instruments, Bedford, U.K.) to give fluctuations <0.015 mbar.

A Commodore microcomputer (CBM 4032, Santa Clara, CA, U.S.A.), interfaced with a 12-bit data acquisition card (Sysmod, Paris, France) was used to control the experiment and to collect the data points of the chromatogram at a rate of 100 Hz. The experimental peaks were fitted to the theoretical model using a non-linear

least-square fit program, written in FORTRAN, with the computer of the Centre Inter Régional de Calcul Electronique, CIRCE (Orsay, France).

## RESULTS

### *Fitting the theoretical curve on the elution peak profile*

We have studied the changes in the elution profiles obtained when increasing amounts of decane are injected into the capillary column at various pressure drops. As usually observed in gas-liquid chromatography, the partition isotherm is concave ( $k''_0 > 0$ ) and produces fronting peaks for large amounts injected.

A least-square fitting of the theoretical elution profile (eqn. 8) was performed on the experimental data of the chromatogram collected by the computer. The correspondence was good for the whole range of concentrations studied, *i.e.* the entire range over which a linear response of the flame-ionization detector is obtained (Fig. 1).

Only four parameters are necessary to characterize the elution profile: the peak size parameter,  $a$ , the retention time at infinite dilution,  $t_R$ , the axial dispersion coefficient of the zone  $D'$ , and the parameter  $\lambda$ , which characterizes the peak slant. These parameters are listed in Table I for a series of injections of increasing mass.

For a given pressure drop, as predicted by the model, the values of  $t_R$ ,  $\lambda$ , and  $D'$  are independent of sample size.

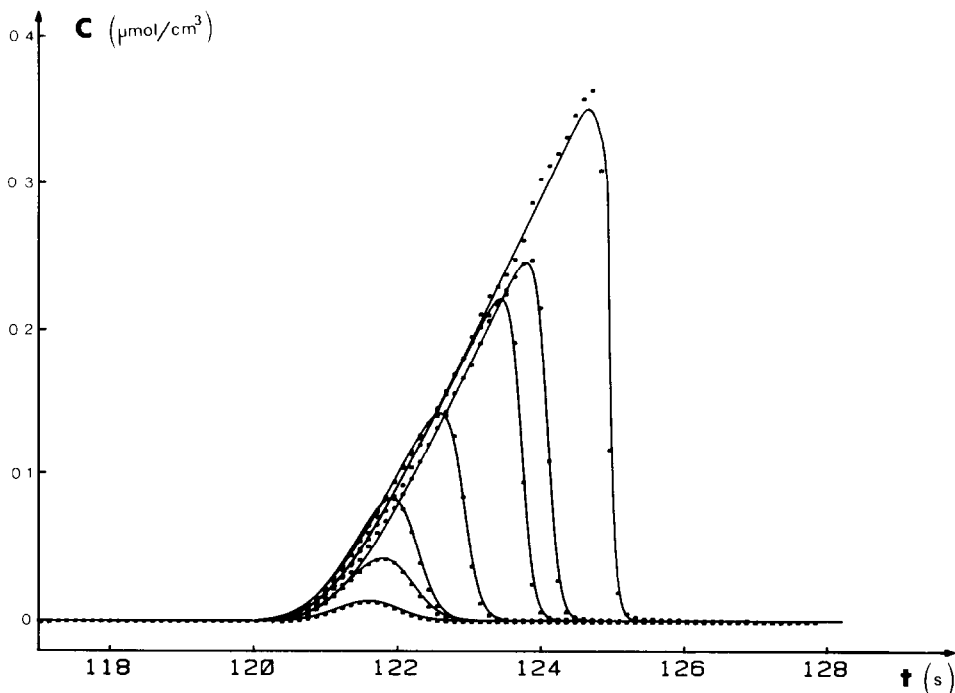


Fig. 1. Best fit of the theoretical profile (eqn. 8) to experimental elution peaks for *n*-decane. Computer data acquisition rate, 50 Hz; pressure drop, 600 mbar.

TABLE I  
 INFLUENCE OF SAMPLE SIZE ON THE PARAMETERS OF THE DECANE PEAK PROFILE

$\Delta P$ (bar)	$m$ ( $\mu\text{g}$ )	$t_M$ (s)	$C_M$ ( $\mu\text{mol/ml}$ )	$a$ ( $s \cdot \mu\text{mol/ml}$ )	$t_R$ (s)	$D'$ ( $\text{cm}^2/\text{s}$ )	$H_0$ (mm)	$\lambda$ ( $\mu\text{mol/ml}$ ) <sup>-1</sup>	$\mu$	$S$
0.4	0.02	182.30	0.059	0.010	182.20	0.17	0.31	0.073	0.27	0.986
	0.55	183.90	0.128	0.258	182.20	0.17	0.31	0.073	6.63	0.502
	1.09	185.20	0.211	0.510	182.20	0.21	0.38	0.078	11.36	0.373
	2.06	186.80	0.307	0.970	182.20	0.23	0.42	0.078	19.69	0.241
0.6	0.05	121.60	0.012	0.013	121.50	0.21	0.26	0.070	0.61	0.931
	0.15	121.80	0.039	0.044	121.50	0.23	0.28	0.066	1.70	0.804
	0.29	121.90	0.076	0.085	121.30	0.21	0.25	0.070	3.89	0.656
	0.60	122.60	0.126	0.172	121.30	0.23	0.28	0.086	8.78	0.426
	1.10	123.50	0.198	0.317	121.30	0.23	0.28	0.086	16.15	0.285
	1.34	123.80	0.219	0.387	121.50	0.24	0.29	0.084	17.58	0.264
0.8	1.75	124.50	0.271	0.504	121.60	0.23	0.28	0.086	25.61	0.196
	0.03	91.80	0.007	0.006	91.70	0.32	0.29	0.075	0.36	0.961
	0.23	92.00	0.048	0.044	91.60	0.32	0.29	0.102	3.29	0.713
	0.40	92.30	0.078	0.076	91.60	0.32	0.29	0.102	5.66	0.561
1.0	1.16	93.30	0.178	0.216	91.60	0.39	0.28	0.105	17.23	0.265
	1.76	93.70	0.231	0.329	91.50	0.31	0.28	0.105	26.29	0.189
	0.03	73.96	0.006	0.005	73.92	0.43	0.32	0.091	0.35	0.984
	0.05	73.95	0.011	0.008	73.82	0.41	0.30	0.125	0.89	0.898
	0.08	73.91	0.017	0.012	73.80	0.40	0.30	0.102	1.13	0.855
	0.16	73.98	0.032	0.023	73.74	0.40	0.29	0.102	2.17	0.766
	0.22	74.20	0.043	0.032	73.81	0.41	0.30	0.125	3.55	0.670
	0.41	74.40	0.078	0.061	73.78	0.41	0.30	0.106	5.65	0.568
1.12	0.56	74.45	0.104	0.083	73.68	0.39	0.29	0.106	8.17	0.442
	1.12	75.02	0.168	0.167	73.74	0.41	0.30	0.106	15.58	0.292
	1.48	75.32	0.198	0.220	73.77	0.41	0.30	0.106	20.48	0.242

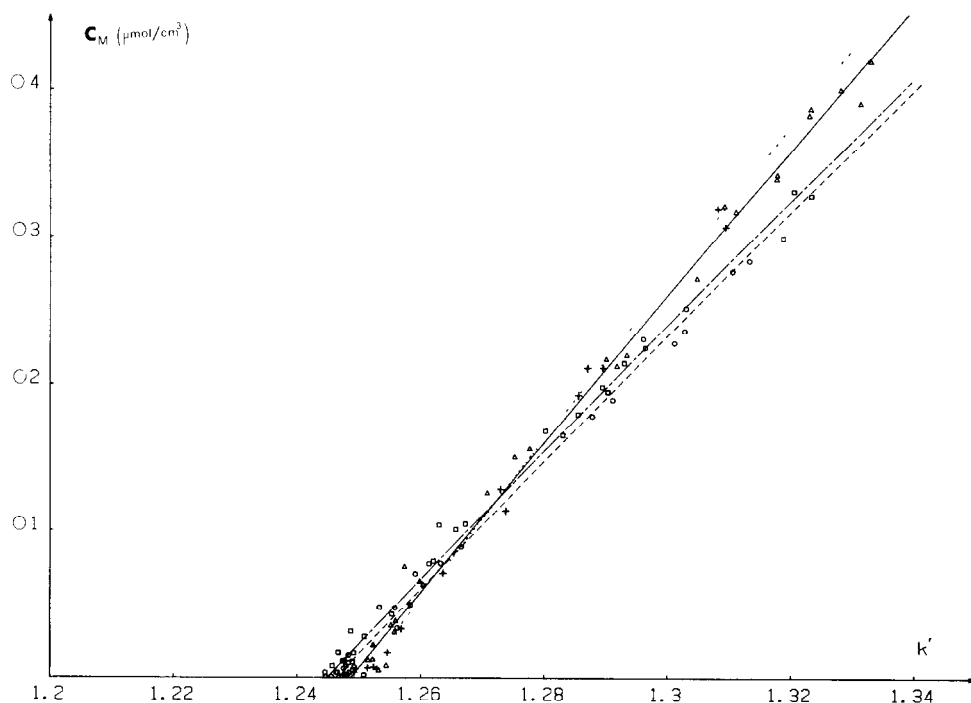


Fig. 2. Variation of the retention time of the peak maximum with the concentration of decane. Pressure drop: (+) 400 mbar; ( $\Delta$ ) 600 mbar; ( $\square$ ) 800 mbar; ( $\circ$ ) 1000 mbar.

#### *Plot of the retention time of the peak maximum vs. sample size*

From the plot of the concentration at peak maximum *vs.* the retention time at peak maximum, it is easy to obtain two of the parameters, characterizing the elution peak by a least-square fitting of eqn. 16 to experimental data,  $t_R$  and  $\lambda$ . In Fig. 2, we have plotted  $C_M$  as a function of  $k' = t_M/t_0 - 1$ , in order to show in one figure the results obtained at various pressure drops.

To a good approximation, the variations of the peak apex are well represented by a straight line (eqn. 17). The scattering of the experimental values of retention times arises from the lack of stability of the flow at the column inlet, since turbulent conditions are necessary to operate the fluidic devices. Therefore, the relative confidence intervals for  $t_R$  and  $\lambda$  determinations are 0.05% and 5%, respectively. The apex locus method shows that it is valid to approximate the sorption isotherm by a parabola on the entire concentration range studied. Moreover, within experimental error, the values of  $t_R$  and  $\lambda$  deduced from the apex locus method (Table II) are in good agreement with those obtained by the peak fitting method (Table I). This agreement proves the validity of using an elution peak model that is based on an expansion of the sorption isotherm to its second term.

#### DISCUSSION

The peak elution model (eqn. 8) provides a good representation of the exper-

TABLE II  
 DETERMINATION OF THE PEAK SLANT COEFFICIENT,  $\lambda$ , BY THE APEX LOCUS METHOD AND CALCULATED CONTRIBUTION OF THE  
 SORPTION EFFECT,  $\lambda_s$

Solute	$\Delta p$ (bar)	$\bar{p}$ bar	$t_0$ (s)	$t_R$ (s)	$\lambda$ (ml/mmol)	$\lambda_s$ (ml/mmol)	$k'_0$ —	$k''_0$ (mmol <sup>-1</sup> )
Decane	0.4	1.2	80.9	182.10 ± 0.10	80 ± 5	-28.00	1.251	248
	0.6	1.3	54.0	121.40 ± 0.10	86 ± 2	-25.50	1.248	256
	0.8	1.5	40.8	91.65 ± 0.05	100 ± 4	-23.40	1.246	283
	1.0	1.6	32.9	73.85 ± 0.05	100 ± 4	-21.50	1.245	278
Pentane	0.6	1.3	54.0	56.35 ± 0.05	-0.82 ± 0.04	-1.94	0.044	1.15
	0.8	1.5	40.8	42.40 ± 0.05	-0.76 ± 0.08	-1.58	0.039	0.89
	1.0	1.6	32.9	34.25 ± 0.05	-0.55 ± 0.05	-1.53	0.041	1.01



imental elution profiles observed in capillary gas chromatography. The theory of non-linear chromatography at moderate concentrations, which leads to a four-parameter equation of the peak profiles, takes into account the non-linearity of the sorption isotherm, the dispersion of the elution band, and the sorption effect. It is based on several assumptions: a parabolic sorption isotherm, a Dirac pulse for the injection signal, ideality of the gas phase, a constant pressure throughout the column, and a dispersion effect independent of the solute concentration. The limits of the applicability of the model are examined by discussing the various effects that determine the peak profiles.

#### *The injection signal function*

The shape of the injection signal obtained by the fluidic injection gate is roughly triangular with a width at half-peak height of 30 ms. It was kept constant throughout this study, independent of the amount of solute injected. Moreover, it was determined that the injection of large concentrations of solutes has no influence on the peak-broadening of an unretained compound (methane was always injected at the same time as the solute vapor).

The contribution of the injection system to peak variance<sup>10</sup> is small ( $\tau^2/6 = 150 \text{ ms}^2$ ) and, in any case, induces no asymmetric effect. Since the standard deviation of the narrowest peak of decane studied was 300 ms, the contribution of the injection system to the peak broadening is less than 0.5%. This proves that it is valid to represent the injection signal by a Dirac function.

#### *Peak-size parameter, $a$*

The peak size parameter,  $a$ , is always larger than the effective peak area,  $A_T$ . It approaches the  $A_T$  value when  $\lambda C_M \ll 1$ . In the concentration range studied in this work,  $\lambda C_M$  never exceeded 0.04 (Table I).

The deviations between the peak parameter,  $a$ , and the actual peak area,  $A_T$ , may be used to estimate the concentration range over which the theoretical model is valid. For the largest injected masses of decane, the differences are lower than 0.2% and, therefore, it is valid to use eqn. 8 to represent the elution profile in the whole domain of concentrations studied in this work.

#### *Dispersion coefficient*

Within experimental error, the dispersion coefficient of the solute zone,  $D'$ , is independent of sample size (Table I). This is in good agreement with the hypothesis made in establishing the general mass-balance equations of chromatography (eqn. 1), which assume that the dispersion coefficient of the zone is independent of solute concentration.

$D'$  is related to the classical height equivalent to a theoretical plate (HETP), measured at infinite dilution:

$$H_0 = 2t_R D' / L \quad (18)$$

Therefore,  $D'$  varies in a similar manner as  $H_0$  with the carrier-gas velocities according to the classical HETP curves. The determination of  $D'$  by fitting the theoretical model to experimental peaks may be useful to measure the HETP at infinite dilution

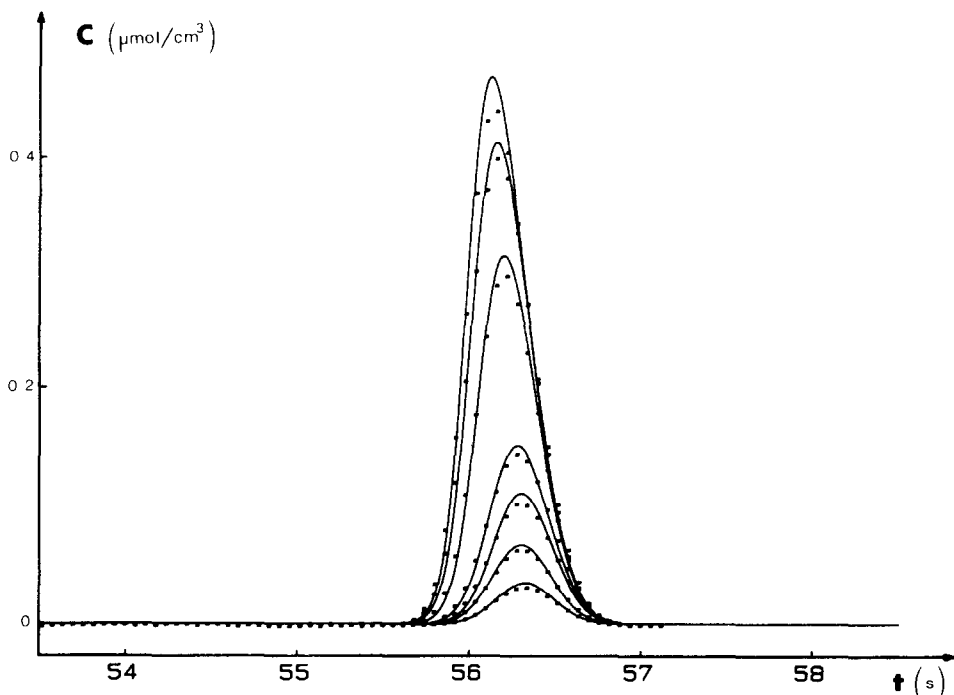


Fig. 3. Best fit of the theoretical profile (eqn. 8) to experimental elution peaks for *n*-pentane (same experimental conditions as in Fig. 1)

of asymmetrically overloaded peaks, for example when the symmetric signals obtained at low concentration vanish into the base-line noise.

#### *Isotherm effect*

The values of the parameters  $t_R$  and  $\lambda$  permit the calculation of the slope,  $k'_0$ , and the curvature of the equilibrium isotherm,  $k''_0$ , at the origin, if, in the concentration range studied, the isotherm can be approximated by a parabola. We have already shown that this hypothesis is valid since we have determined that the experimental apex locus plot is in good agreement with eqn. 15.

The values of  $k'_0$  and  $k''_0$  are obtained from  $t_R$  and  $\lambda$  values. The second derivative at the origin,  $k''_0$ , is calculated from the value of the peak slant coefficient and takes into account the contribution of the sorption effect (eqns. 5 and 11).

Small but significant variations of  $k'_0$  and  $k''_0$  with pressure drop were observed, and  $k'_0$  slightly decreases with increasing (mean) column pressure, in agreement with the theory developed by Desty *et al.*<sup>11</sup>. A corrective term for  $k'_0$  accounts for the non-ideality of the gaseous phase and is equal to  $(B_{12} - v_1^0)/RT$  where  $B_{12}$  is the second virial coefficient of the solute in the gas phase and  $v_1^0$  is the partial volume of the solute at infinite dilution. The variations of  $k''_0$  with column pressure drop may have the same origin, since the model does not account for non-ideality of the gaseous phase and assumes a constant pressure equal to the mean column pressure throughout the column.

*Sorption effect*

The sorption effect is included in the term  $\lambda_s = -2k'_0RT/\bar{p}$ . It will tend to skew the decane elution peak, since its sign is opposite of that of the isotherm effect. Its influence on peak distortions is important, since it contributes up to 30% of the total peak slant coefficient.

The validity of the correction for the sorption effect could be tested with chromatographic systems where the isotherm effect is reduced or eliminated. With the capillary column used in this work, the isotherm effect is important, because the amount of the liquid stationary phase is low. Therefore, only when large amounts of compounds with small capacity ratios are injected will the peak distortions mainly be due to a major sorption effect.

For *n*-pentane at 100°C, the isotherm effect is small and the variations of the peak shape with the amount injected are mainly caused by a sorption effect, which tends to skew the elution peak (Fig. 3). In Table III, the values of the parameters corresponding to the peak adjustments of Fig. 3 are reported.

From the plot of the maximum concentration vs. maximum retention time at various pressure drops, we have obtained absolute values of the peak slant coefficients which are lower than those of the theoretical peak slant coefficient,  $\lambda_s$ , corresponding to a pure sorption effect. The contribution of the isotherm effect is therefore still important (*i.e.* about half the sorption effect), due to a positive curvature of the equilibrium isotherm.

In agreement with theory, for pentane as a solute, when the sorption effect is the major contribution to  $\lambda$ , the absolute value of the peak slant coefficient decreases by increasing the mean column pressure (Table II). However, the validity of the corrective term for the sorption effect cannot be quantitatively tested in this work, since the isotherm effect should be eliminated or at least known from independent measurements. Moreover, the range of pressure drops under investigation should be larger, with a more precise control, of the carrier-gas flow-rate.

*Characterization of peak asymmetry*

The experimental asymmetry of the peak can be measured from the ratio

$$S = w_1/w_2 \quad (19)$$

TABLE III

INFLUENCE OF SAMPLE SIZE ON THE PARAMETERS OF THE PENTANE PEAK PROFILE

<i>m</i> ( $\mu\text{g}$ )	$t_M$ ( <i>s</i> )	$C_M$ ( $\mu\text{mol/ml}$ )	<i>a</i> ( $\mu\text{mol/ml}$ )	$t_R$ ( <i>s</i> )	$D'$ ( $\text{cm}^2/\text{s}$ )	$\lambda$ ( $\mu\text{mol/ml}$ ) <sup>-1</sup>
0.26	56.33	0.322	0.148	56.34	0.31	0.000699
0.51	56.31	0.653	0.290	56.33	0.32	0.000728
0.85	56.34	1.055	0.482	56.35	0.32	0.000728
1.17	56.29	1.484	0.668	56.34	0.33	0.000699
2.41	56.21	3.034	1.370	56.33	0.32	0.000728
3.21	56.17	4.046	1.828	56.32	0.33	0.000699
3.63	56.14	4.485	2.067	56.32	0.32	0.000728

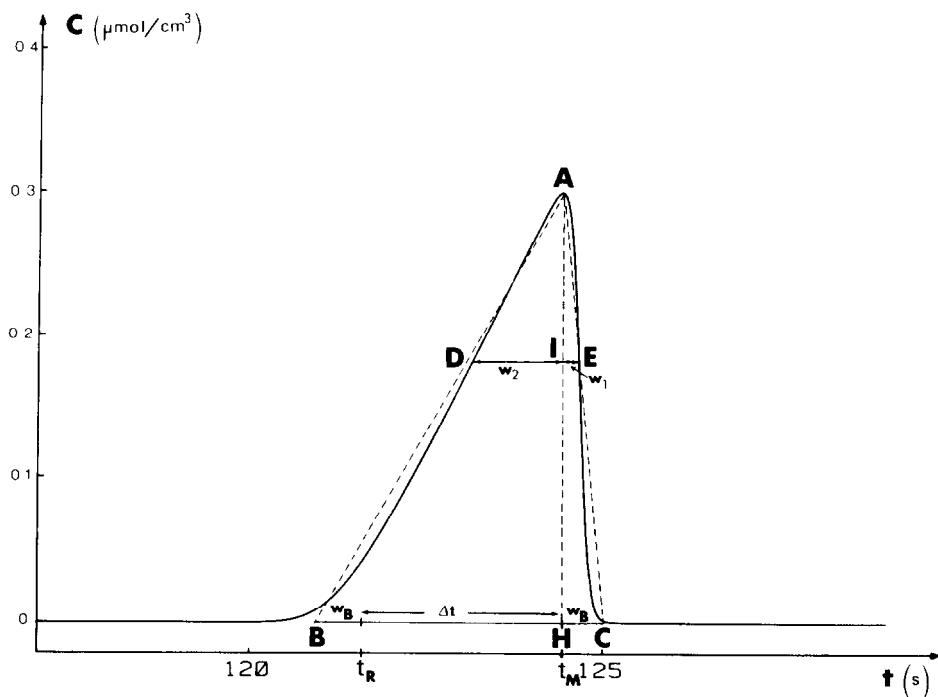


Fig. 4. Triangular diagram, representing an elution peak.

where  $w_2$  and  $w_1$  are the half-widths, measured at a given fraction of the peak height, before and after the elution time of peak maximum  $t_M$ , respectively. We measured  $w_2$  and  $w_1$  at 0.606 of the maximum peak height,  $C_M$ , since for a Gaussian peak the widths  $w_1$  and  $w_2$  are then equal to the standard deviation,  $\sigma_0$ .

We have shown, in a previous paper<sup>12</sup> that the parameter  $\mu$  of the theoretical model is directly related to the peak asymmetry of tailing peaks observed in liquid chromatography where the asymmetry ratio,  $S$ , is larger than unity. The same procedure will be applied here with a fronting peak where  $S < 1$  to demonstrate the existence of a relationship between  $\mu$  and peak asymmetry.

We assume that the elution peak (maximum abscissa,  $t_M$  and  $C_M$ ) can be approximated by a triangle (Fig. 4) of height,  $AH = C_m$ , and of basis,  $BC$ , with  $HC = w_B = w_1/0.394$ , and  $BC = \Delta t + w_B$ , where  $t = t_M - t_R$  ( $t_R$  is the retention time at infinite dilution) and where  $w_1 = IE$  and  $w_2 = ID$ . The location of  $C$  is such that  $A$ ,  $E$ , and  $C$  lie on the same straight line. The theoretical asymmetry factor,  $S_0$ , calculated at the basis of the triangle  $ABC$  is related to the triangle area,  $A$ , and to the peak slant coefficient,  $\lambda$ , according to mathematical procedures analogous to those previously developed<sup>12</sup>:

$$\frac{1}{S_0} = \sqrt{1 + 2 \frac{A\lambda t_R}{w_B^2}} \quad (20)$$

The peak asymmetry,  $S_0$ , of the triangle symbolizing the peak is not rigorously equal to the asymmetry,  $S$ , measured at 0.606 of peak-height, since  $A$ ,  $D$ , and  $B$  are not on

the same straight line. Assuming that the triangle area,  $A$ , is equal to the peak parameter,  $a$ , we obtain a relationship between the asymmetry factor and the peak parameter,  $\mu$ , of a fronting peak:

$$\frac{1}{S_0^2} = 1 + 2 \mu \left( \frac{\sigma_0}{w_B} \right)^2 \tag{21}$$

The plot of  $1/S_0^2$  as a function of  $\mu$  is not strictly a straight line, because the ratio  $\sigma_0/w_B = 0.394 (\sigma_0/w_1)$  varies with  $\mu$ . We have observed (Fig. 5a) that the ratio  $\sigma_0/w_1$  varies linearly with  $\mu$ :

$$\sigma_0/w_1 = \gamma + \delta\mu \tag{22}$$

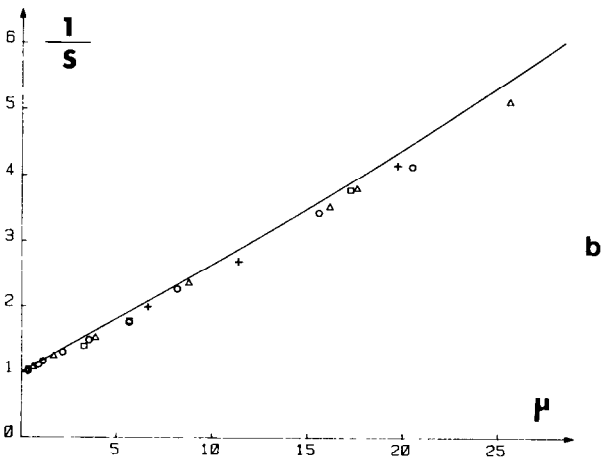
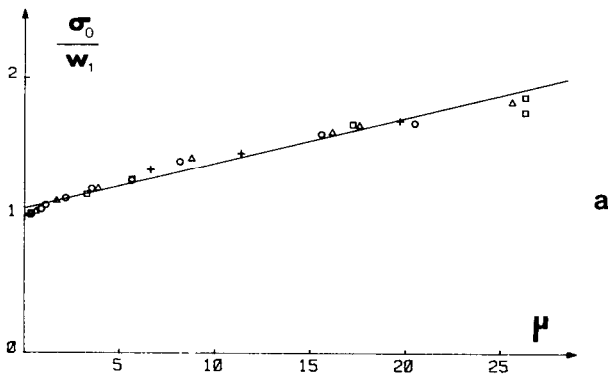


Fig. 5. Variation of the asymmetry of the decane elution peak with the parameter  $\mu$  of the elution model. a) Plot of  $\sigma_0/w_1$  vs.  $\mu$ :  $\sigma_0/w_1 = 1.06 + 0.033 \mu$  (solid line) b) Plot of  $1/S$  vs.  $\mu$ :  $1/S = \sqrt{1 + 0.31 \mu (1.06 + 0.033\mu)^2}$  (solid line) Column temperature,  $100^\circ\text{C}$ ; carrier gas, helium. pressure drop, (+) 400 mbar; ( $\Delta$ ) 600 mbar; ( $\square$ ) 800 mbar; ( $\circ$ ) 1000 mbar.

where  $\gamma = 1.057$  and  $\delta = 0.033$ . In this figure we show the experimental values from peaks obtained by injecting various sample sizes at various pressure drops.

Therefore, the variation of  $S_0$  with  $\mu$  is well represented by the equation

$$\frac{1}{S_0^2} - 1 = 0.31 \mu(\gamma + \delta\mu)^2 \quad (23)$$

Excellent agreement is observed between the calculated asymmetry factor,  $S_0$  (drawn line in Fig. 5) and the experimental one,  $S$ , specially if it is kept in mind that the experimental peak asymmetries are measured for various masses injected at various carrier-gas velocities.

The relationship involving the asymmetry ratio and the peak parameter,  $\mu$ , is useful for relating the degree of asymmetry of an overloaded peak to the various characteristics of the chromatographic experiment. From the expression for  $\mu$  (eqn. 14) we deduce

$$\mu = a\lambda L/t_R H_0 \quad (24)$$

where  $H_0$  is the column HETP at infinite dilution. Since the amount injected,  $Q$ , is related to the peak area,  $a$ , and to the flow rate,  $F$ ,  $\mu$  equals

$$\mu = \frac{Q\lambda L}{F t_R H_0} = \frac{4 Q}{\pi d^2 H_0} \frac{\lambda}{(1 + k'_0)} \quad (25)$$

where  $\pi d^2/4$  is the column cross-section.

We define  $\mu_0$  as the proportionality factor relating  $\mu$  to the mass injected

$$\mu_0 = \frac{\mu}{Q} = \frac{4}{\pi d^2 H_0} \frac{\lambda}{(1 + k'_0)} \quad (26)$$

If we neglect the sorption effect,  $\mu_0$  will only depend on the characteristics of the capillary column and on the nature of the solute and the stationary phase

$$\mu_0 \approx \frac{4}{\pi d^2 H_0} \frac{k'_0 V_0}{(1 + k'_0)^2} \approx \frac{1}{\pi d^2 H_0} \frac{\beta V_s/V_0}{(1 + \alpha V_s/V_0)^2} \quad (27)$$

Since  $V_s/V_0 \approx 4d_f/d$ , where  $d_f$  is the film thickness, we obtain for  $\mu_0$

$$\mu_0 \approx \frac{16}{\pi d^3 H_0} \frac{\beta d_f}{(1 + 4\alpha d_f/d)^2} \quad (28)$$

Interesting conclusions can be derived from the above equation. For the same amount injected, the parameter  $\mu$  and, therefore, the asymmetry due to column overloading is independent of column length. It is also independent of flow-rate, if we assume that the variations of  $H_0$  with carrier-gas velocities are not important, *i.e.* the experiments are carried out around the minimum of the HETP curve.

Asymmetries due to column overloading will increase, if the diameter of the

capillary column is decreased, and for large values of  $k'$ , with decreasing film thickness. These phenomena have been observed with small-diameter capillary columns for fast analysis in capillary GC<sup>13,14</sup>.

## CONCLUSION

The model for asymmetric chromatographic elution peaks, derived for moderate concentrations, accounts well for the elution profiles observed with overloaded capillary columns, when tailing due to extra-column contributions or kinetic effects has been eliminated. The four-parameter model may be useful, with strongly overlapping peaks, for identifying components and for extracting information about their composition, even if the column is overloaded.

The factor  $\mu_0$  (eqn. 26), which characterizes peak asymmetry, is easily measured from the value of the peak slant coefficient obtained by the apex locus method. It defines the degree of overloading of a capillary column for a given solute at a given temperature. It is useful for comparing stationary phases and the various manufacturing and coating procedures for capillary columns.

## LIST OF SYMBOLS

- $a$  : peak size parameter
- $A_T$  : peak area
- $A$  : area of the triangle symbolizing the peak
- $B_{12}$  : second virial coefficient of the solute in the gas phase
- $C$  : concentration of solute in the carrier gas
- $C_M$  : solute concentration at peak maximum
- $d$  : capillary column diameter
- $d_f$  : stationary film thickness
- $D$  : global diffusion coefficient
- $D'$  : auxiliary variable  $D' = D/(1 + k')$
- $F$  : flow-rate
- $H_0$  : limit plate height for zero sample size
- $k'$  : column capacity factor
- $k'_0$  : limiting value of  $k'$  for zero sample size:  $k'_0 = (t_R - t_0)/t_0$
- $k''_0$  : second coefficient of the two-term expansion of  $k'$  (eqn. 7)
- $n_A^S$  : number of moles of solute in the stationary phase at equilibrium
- $n_A^G$  : number of moles of solute in the gas phase at equilibrium
- $L$  : column length
- $\bar{p}$  : mean column pressure
- $Q$  : amount injected
- $R$  : ideal gas constant
- $S$  : experimental asymmetry factor at 0.606 of peak height (eqn. 19)
- $S_0$  : theoretical asymmetry factor calculated at the basis of the triangle symbolizing the peak (eqn. 20)
- $T$  : absolute temperature
- $t$  : time; time origin at the injection of the solute
- $t_0$  : retention time of a non-retained compound

- $t_M$  : retention time of peak maximum  
 $t_R$  : limit retention time for zero sample size  
 $U$  : auxiliary variable  $U = u_0/(1 + k'_0)$   
 $u_0$  : outlet carrier-gas velocity  
 $v_1^0$  : partial molar volume of the solute at infinite dilution  
 $V_0$  : volume of the gaseous phase  
 $V_S$  : volume of the stationary phase  
 $w_1$  : part of peak width after maximum elution  
 $w_2$  : part of peak width prior to maximum elution  
 $X$  : mole fraction of the solute in the gas phase  
 $z$  : abscissa along the column  
 $\alpha, \beta$  : coefficients of parabolic isotherm (eqn. 6)  
 $\gamma, \delta$  : coefficients of the linear variation of  $\sigma_0$  with  $\mu$  (eqn. 22)  
 $\xi$  : auxiliary variable  $\xi = z - Ut$   
 $\lambda$  : peak slant coefficient (eqn. 11)  
 $\lambda_S$  : contribution of the sorption effect to the peak slant coefficient (eqn. 5)  
 $\mu$  : auxiliary variable characteristic of peak asymmetry (eqn. 14)  
 $\mu_0$  : proportionality factor characteristic of peak asymmetry (eqn. 26)  
 $\sigma_0$  : standard deviation of the Gaussian profile obtained for zero sample size  
 $\tau$  : width of the injection triangular signal.

## REFERENCES

- 1 A. H. Anderson, T. C. Gibb and A. B. Littlewood, *J. Chromatogr. Sci.*, 8 (1970) 640.
- 2 E. Grushka, *Anal. Chem.*, 44 (1972) 1733.
- 3 J. C. Giddings, *Anal. Chem.*, 35 (1963) 1999.
- 4 J. Villermaux, *J. Chromatogr. Sci.*, 12 (1974) 822.
- 5 A. Jaulmes, A. Ladurelli, C. Vidal-Madjar and G. Guiochon, *J. Phys. Chem.*, 88 (1984) 5379.
- 6 A. Jaulmes, C. Vidal-Madjar, M. Gaspar and G. Guiochon, *J. Phys. Chem.*, 88 (1984) 5385.
- 7 P. Cardot, I. Ignatiadis, A. Jaulmes, C. Vidal-Madjar and G. Guiochon, *J. High Resolut. Chromatogr. Chromatogr. Commun.* 8 (1985) 591.
- 8 J. R. Conder and J. H. Purnell, *Trans. Farad. Soc.*, 64 (1968) 3100.
- 9 G. Houghton, *J. Phys. Chem.*, 67 (1963) 84.
- 10 G. Gaspar, R. Annino, C. Vidal-Madjar and G. Guiochon, *Anal. Chem.*, 50, (1978) 1512.
- 11 D. H. Desty, A. Goldup, G. R. Luckhurst and W. T. Swanton, in M. van Swaay (Editor), *Gas Chromatography*, 1962, Butterworths, London, 1962, p. 67.
- 12 A. Jaulmes, M. J. Gonzalez, C. Vidal-Madjar and G. Guiochon, *J. Chromatogr.*, 386 (1987) 333.
- 13 C. P. M. Schutjes, E. A. Venneer, J. A. Rijks and C. A. Cramers, *J. Chromatogr.*, 253 (1982) 1.
- 14 C. P. M. Schutjes, C. A. Cramers, C. Vidal-Madjar and G. Guiochon, *J. Chromatogr.*, 279 (1983) 269.